Research article

The PDIA3-STAT3 protein complex regulates IBS formation and development via CTSS/MHC-II pathway-mediated intestinal inflammation

Chunyan Weng [a], Jingli Xu [a], Xiao Ying [b], Shaopeng Sun [a], Yue Hu [a], Xi Wang [a,c], Chenghai He [d], Bin Lu [a,**], Meng Li [a,*]

[a] *Department of Gastroenterology, The First Affiliated Hospital of Zhejiang Chinese Medical University (Zhejiang Provincial Hospital of Chinese Medicine), Hangzhou 310000, Zhejiang Province, China*
[b] *Department of Gastroenterology, The First People's Hospital of Yongkang, Jinhua 321300, Zhejiang Province, China*
[c] *Key Laboratory of Digestive Pathophysiology of Zhejiang Province, the First Affiliated Hospital of Zhejiang Chinese Medical University, Zhejiang Chinese Medical University, Hangzhou, 310006, China*
[d] *Department of Internal Medicine, The Affiliated Hospital of Hangzhou Normal University, 126 Wenzhou Road, Hangzhou, Zhejiang Province, China*

ARTICLE INFO

ABSTRACT

Irritable bowel syndrome (IBS) is a persistent functional gastrointestinal disorder characterised by abdominal pain and altered patterns of defecation. This study aims to clarify an increase in the expression and interaction of protein disulfide-isomerase A3 (PDIA3) and Signal Transducer and Activator of Transcription 3 (STAT3) within the membrane of dendritic cells (DCs) from individuals with IBS. Mechanistically, the heightened interaction between PDIA3 and STAT3 at the DC membrane results in reduced translocation of phosphorylated STAT3 (p-STAT3) into the nucleus. The reduction of p-STAT3 to nuclear transport subsequently increased the levels of cathepsin S (CTSS) and major histocompatibility complex class II (MHC-II). Consequently, activated DCs promote $CD4^+$ T cell proliferation and cytokine secretion, including interleukin-4 (IL-4), interleukin-6 (IL-6), interleukin-9 (IL-9), and tumour necrosis factor-alpha (TNF-α), thereby contributing to the development of IBS. Importantly, the downregulation of PDIA3 and the administration of punicalagin (Pun), a crucial active compound found in pomegranate peel, alleviate IBS symptoms in rats, such as increased visceral hypersensitivity and abnormal stool characteristics. Collectively, these findings highlight the involvement of the PDIA3-STAT3 protein complex in IBS, providing a novel perspective on the modulation of immune and inflammatory responses. Additionally, this research advances our understanding of the role and mechanisms of PDIA3 inhibitors, presenting new therapeutic possibilities for managing IBS.

1. Introduction

Irritable bowel syndrome (IBS) stands as a significant functional gastrointestinal disorder with a substantial global prevalence,

presenting symptoms of pain and disrupted bowel movements in the absence of identifiable organic causes, as outlined in the Rome IV Diagnostic Criteria [1,2]. It affects 5–20 % of the general population and significantly impacts the quality of life. However, our understanding of the underlying pathogenic mechanisms remains limited [3]. Epidemiological investigations have identified various risk factors that either trigger or exacerbate IBS symptoms. These factors include antecedent gastrointestinal infections, psychological stress, immune dysregulation, and dietary elements [4]. Notably, mucosal immune dysfunction stands out among these risk factors and is widely recognised as a key contributor [5].

Within the mucosal immune system, antigen-presenting cells (APCs) play a central role in initiating T cell activation, with dendritic cells (DCs) serving as the principal APCs. Animal studies have underscored the involvement of DCs in the pathogenesis of IBS, as evidenced by the induction of visceral hypersensitivity and T cell activation [6,7]. Previous findings have demonstrated a significant
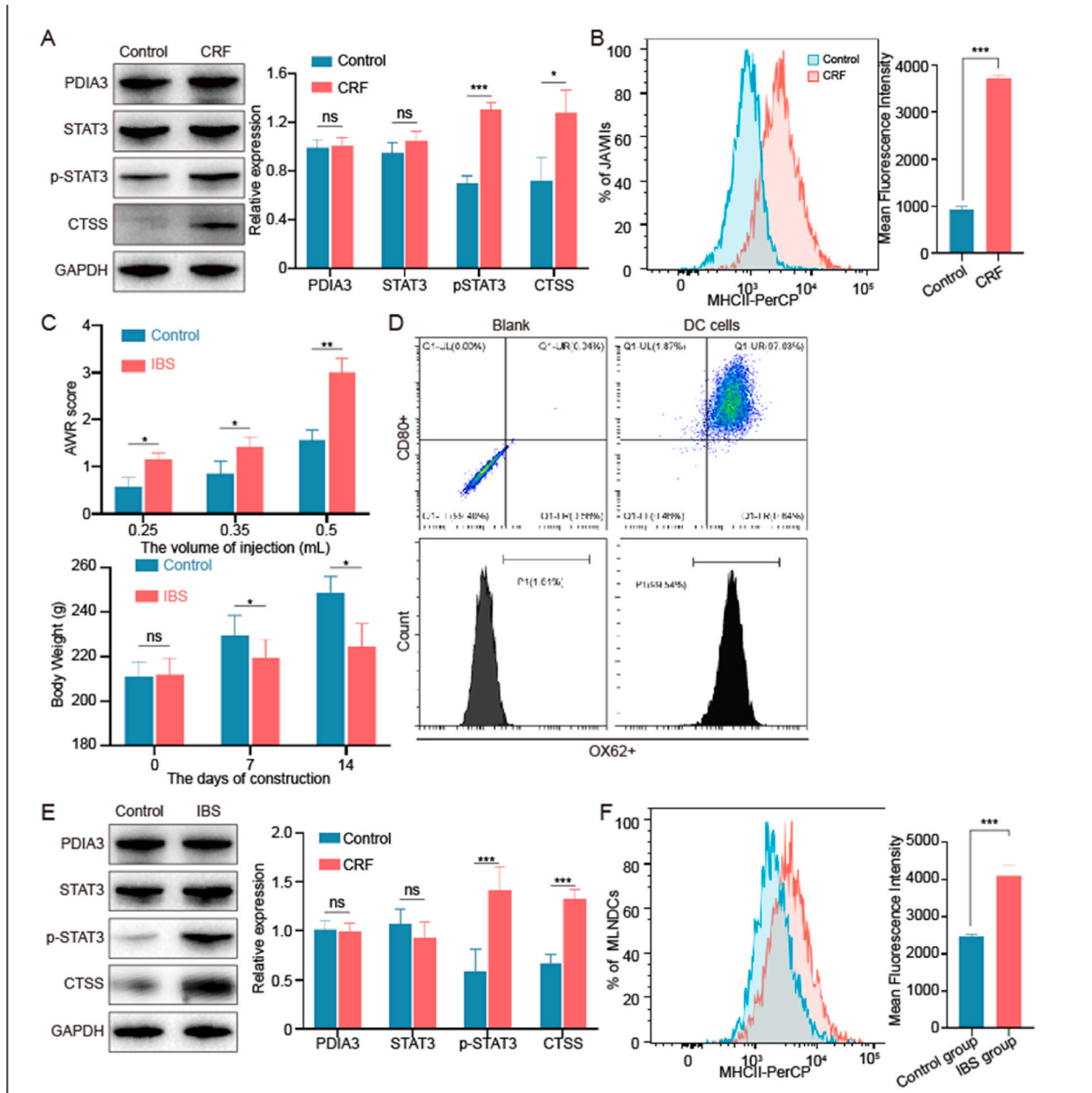

Fig. 1. The correlative expression of proteins both in vivo and in vitro. (A) The effects of CRF (100 nM, 24 h) on the expression of PDIA3, STAT3, P-STAT3, and CTSS in JAWSII cells were assessed by Western blots.(B) Membrane MHC-II expression was determined by flow cytometry analysis.(C) Treatment efficacy was evaluated in IBS rats (n = 6/group) by assessing the body weight of rats at day 0, 7, and 14, as well as AWR scores at pressure stimulations of 0.35 mL, 0.5 mL, and 0.75 mL. (D–E) The correlative expression of proteins in vivo was assessed by Western blots and flow cytometry. Values are presented as means ± SEM. "n.s." indicates no significance, *$P < 0.05$, **$P < 0.01$, ***$P < 0.001$.

increase in dendritic cell (DC) abundance in patients with both IBS and inflammatory biowel disease (IBD), accompanied by the upregulation of mature co-stimulatory molecules, including CD80, CD86, and major histocompatibility complex class II (MHC-II). Simultaneously, there was an elevation in the secretion of inflammatory cytokines, as well as enhanced migration and proliferation of CD4^{+} T cells. These events culminated in the orchestration of Th1 and Th17 inflammatory responses [8]. Furthermore, in our previous study, we confirmed the surface expression of corticotropin-releasing factor (CRF) receptors on DCs within the mouse mesenteric lymph nodes (MLNDCs). Moreover, our findings revealed that CRF has the capacity to alter the phenotype and function of MLNDCs by upregulating the expression levels of surface molecules, such as MHC-II, and enhancing their ability to stimulate T cells [9,10].

In our previous study, we found a significant upregulation of protein disulfide-isomerase A3 (PDIA3), also known as endoplasmic
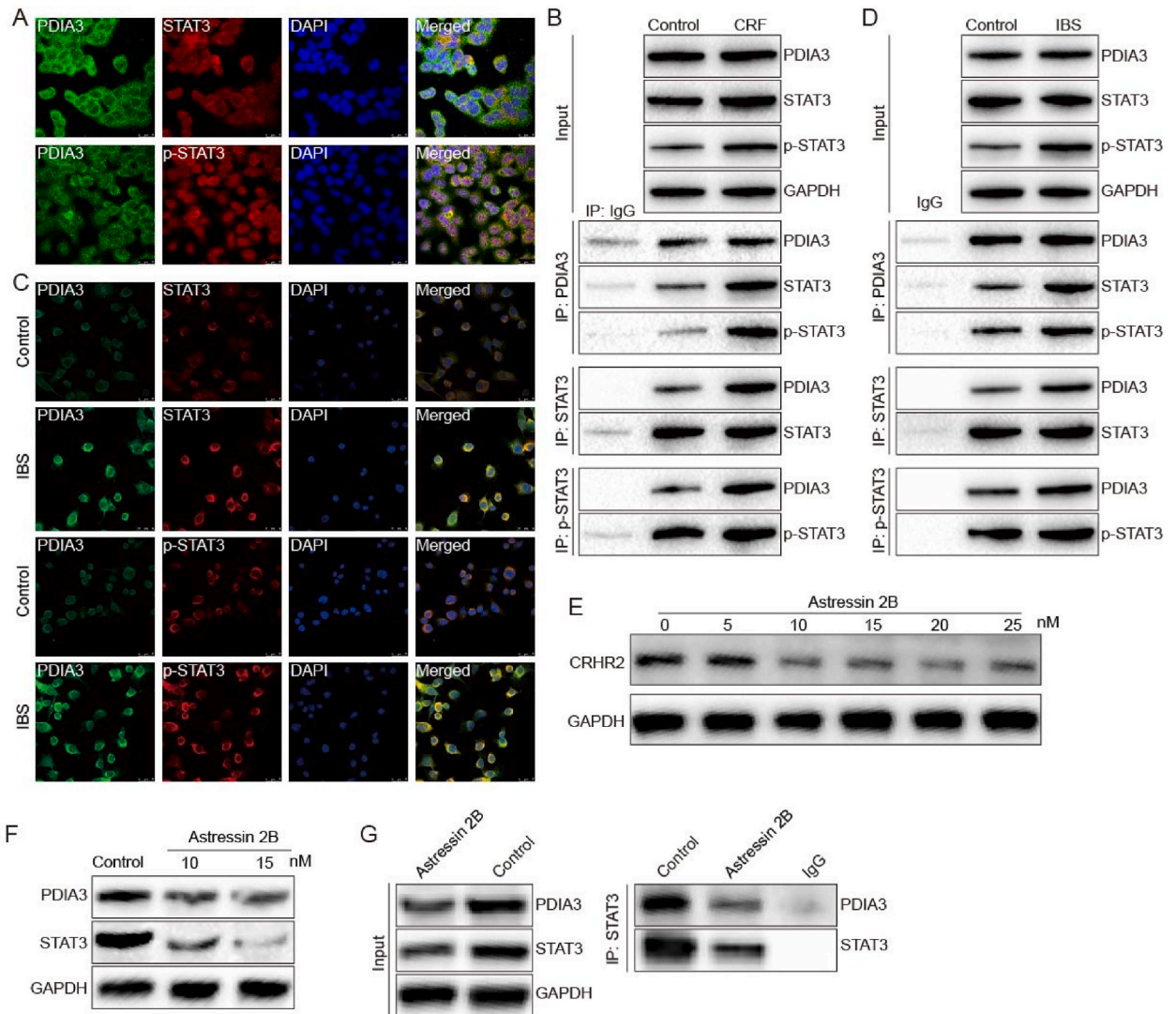

Fig. 2. Association of PDIA3 with STAT3 and its phosphorylation both in vivo and in vitro. (A) Immunofluorescent staining was conducted to observe the colocalization of PDIA3 (green), STAT3/p-STAT3 (red), and the nucleus (DAPI, blue) in vitro. The merged image displayed yellow, indicating colocalization of PDIA3 and STAT3/p-STAT3. (B) Co-immunoprecipitation experiments were carried out using antibodies targeting PDIA3 and STAT3 or p-STAT3. Subsequently, immunoblots were performed to detect PDIA3 and STAT3 or p-STAT3 in vitro. Normal rabbit IgG served as the control. (C) Immunofluorescent staining was performed to assess the colocalization of PDIA3 (green), STAT3/p-STAT3 (red), and the nucleus (DAPI, blue) in both the control and IBS groups. Yellow in the merged image indicated colocalization of PDIA3 and STAT3/p-STAT3. (D) A co-immunoprecipitation assay was executed using anti-PDIA3, anti-STAT3, and their phosphorylated forms. Immunoblotting was then carried out with anti-STAT3 or anti-PDIA3 antibodies, anti-p-STAT3 in vivo, respectively. Normal rabbit IgG was used as the control. (E) Immunoblot analysis of **CRFR** protein in JAWSII cells following Astressin 2B treatment (CRFR inhibitor, 24h) at various concentrations (0, 5, 10, 15, 20, and 25 nM). (F) Immunoblot analysis was conducted on PDIA3 and STAT3 proteins in JAWSII cells after treatment with Astressin 2B at two concentrations (10 and 15 nM). (G) co-immunoprecipitation assay was executed using anti-PDIA3, anti-STAT3, and their phosphorylated forms in JAWSII cells following Astressin 2B treatment at 15 nM concentration. (For interpretation of the references to color in this figure legend, the reader is referred to the Web version of this article.)

reticulum resident protein (ERp57), in the colon mucosa tissues of IBS-afflicted rats [11,12]. Furthermore, we demonstrated that knocking down PDIA3 can alleviate sensitivity by reducing the number of intestinal DCs and the subsequent T cell proliferation induced by these cells [13]. It's noteworthy that recent observations have revealed its presence on the cell surface, where it interacts with specific membrane proteins. Signal transducer and activator of transcription 3 (STAT3), a crucial transcription factor [13], has been shown to co-localise with PDIA3 and is implicated in various cellular processes [14,15]. However, limited attention has been given to understanding the role of the PDIA3-STAT3 complex in mesenteric lymph node dendritic cells (MLNDCs).

In this study, we investigated the impact of the PDIA3-STAT3 complex on DC activation and visceral sensitivity in rat models of IBS. Our aim was to enhance our understanding of the mechanistic aspects of IBS.

2. Results

2.1. Phosphorylated STAT3 (p-STAT3) was up-regulated in DCs of IBS model

To investigate the protein levels of DCs in IBS patients, we employed CRF treatment on JAWSII cells to simulate IBS occurrence, as previously outlined [16]. As shown in Fig. 1A, the expression levels of PDIA3 and STAT3 remained unchanged after CRF treatment. Interestingly, the expressions of p-STAT3 and cathepsin S (CTSS), a potential downstream target of p-STAT3 known to regulate MHC-II expression [17], were upregulated following CRF treatment. Flow cytometry analysis confirmed an increase in membrane MHC-II after CRF treatment (Fig. 1B). It's worth noting that previous studies [17–19] reported that p-STAT3 could downregulate CTSS at the mRNA
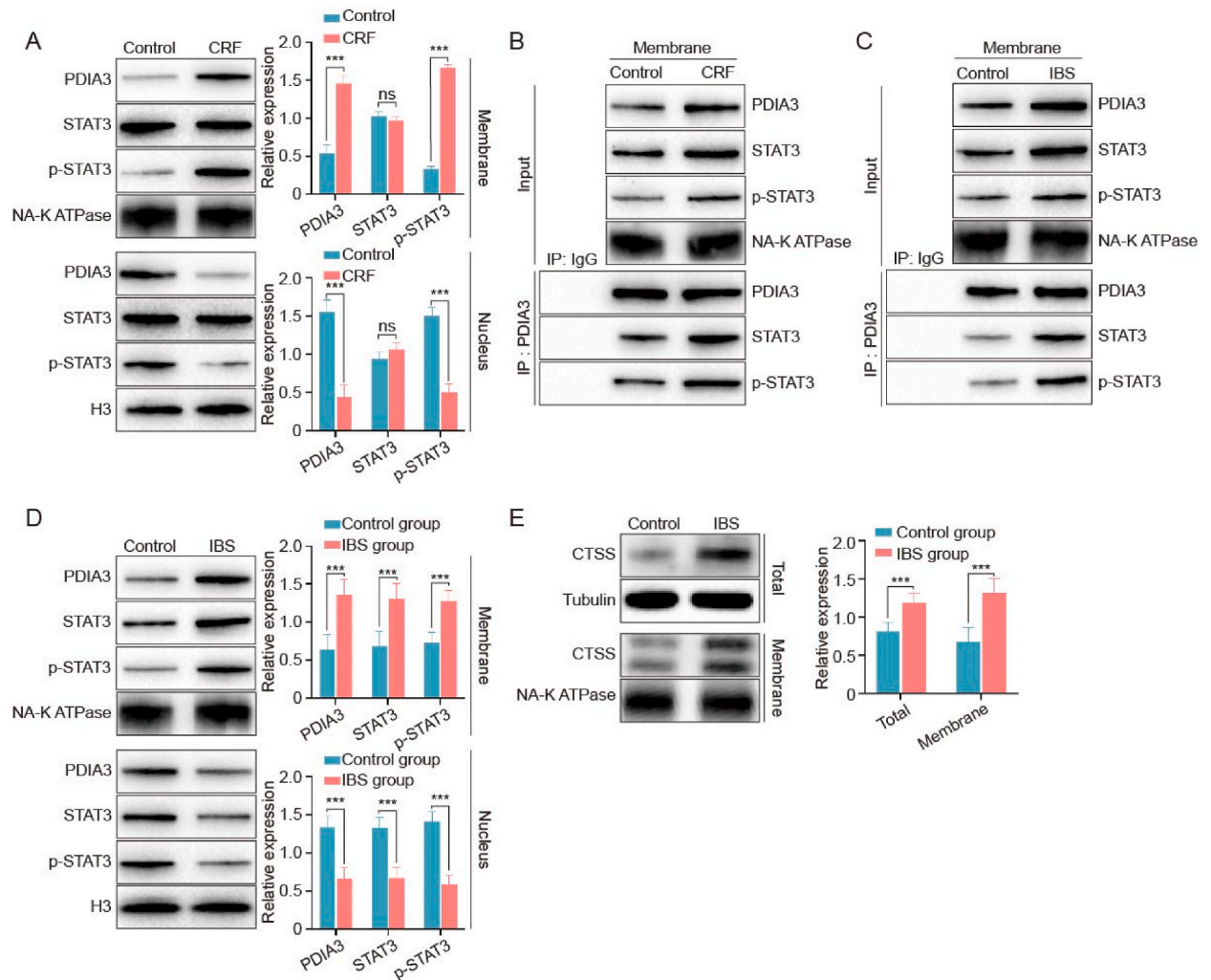

Fig. 3. (A) Immunoblot analysis of correlated proteins in the membrane and nucleus of JAWSII cells following CRF treatment (100 nM, 24 h). (B and C) Detection of the association of PDIA3 with STAT3 and its phosphorylation on the DC cell membrane through in vitro and in vivo co-immunoprecipitation. (D) Immunoblot analysis of correlated proteins in the membrane and nucleus in vivo. Values represent means ± SEM. "n. s." denotes no significance, *P < 0.05, **P < 0.01, ***P < 0.001.

level, which contrasts with our findings.

To establish a stable animal model of IBS, we selected rats for this study and followed established protocols. IBS-afflicted rats exhibited a significant elevation in the abdominal withdrawal reflex (AWR) score, a metric used to evaluate visceral hypersensitivity [20], in comparison to the control group (Fig. 1C). Furthermore, IBS rats displayed characteristic symptoms of IBS, including weight loss and growth retardation (Fig. 1C). Subsequently, we isolated DCs in the MLNDCs using a magnetic kit, following the provided guidelines, and the purity of the sorted DCs is depicted in Fig. 1D. In alignment with the findings in JAWSII cells, levels of p-STAT3, CTSS, and MHC-II in MLNDCs were elevated in the IBS group, while PDIA3 and STAT3 levels remained comparable (Fig. 1E and F).

In summary, these results emphasise the intricate regulation of p-STAT3 expression in DCs in the pathogenesis of IBS.

2.2. Interaction and Co-localisation of PDIA3 with STAT3 and p-STAT3 on DC membranes

In light of previous reports on the interaction and co-localisation of STAT3 and PDIA3 [14,15], we conducted co-immunoprecipitation and immunofluorescence analyses to explore their role in DCs. As illustrated in Fig. 2A, dual immunofluorescent staining revealed the co-localisation of PDIA3 (in green) with STAT3 (in red) or p-STAT3 (in red) in JAWSII cells, notably on cell membranes (merge, shown in yellow). Additionally, co-immunoprecipitation assays demonstrated an interaction between PDIA3 and STAT3 or p-STAT3 in JAWSII cells (Fig. 2B), with an increased interaction observed following CRF treatment (Fig. 2B). Consistent with these observations in JAWSII cells, the interaction and co-localisation of PDIA3 with STAT3 or p-STAT3 were corroborated in DCs from MLNDCs (Fig. 2C and D). These findings highlight PDIA3's ability to interact with both STAT3 and p-STAT3, maintaining their co-localisation in DCs.

Furthermore, to explore the role of CRF in the PDIA3-STAT3 complex, we initially treated JAWSII cells with a randomly selected CRFR inhibitor. The results revealed a concentration-dependent expression of CRFR (Fig. 2E). Subsequently, we examined the impact of two concentrations, 10 nM and 15 nM, on the expression of PDIA3 and STAT3. The findings demonstrated a significant decrease in the expression of both PDIA3 and STAT3 (Fig. 2F). Finally, at a concentration of 15 nM, we investigated the inhibitory effects of the CRFR inhibitor on the complex, leading to a pronounced inhibition of the mutual interaction between PDIA3 and STAT3 (Fig. 2G).

2.3. Up-regulation of PDIA3-STAT3/p-STAT3 interaction on DC membranes in the IBS model

To further investigate whether the expression or interaction of PDIA3 and STAT3/p-STAT3 is regulated in the IBS model, we performed membrane and nucleus separation in JASWII cells after CRF treatment and in DCs from IBS rats. Fig. 3A illustrates that CRF upregulated the expressions of PDIA3 and p-STAT3 on the membranes of JAWSII cells, while it decreased their presence in the nucleus. However, the expression of STAT3 remained unchanged. Interestingly, the increased expression of p-STAT3 on the membrane and its decreased expression in the nucleus plausibly explained the upregulation of CTSS, even though the total expression of p-STAT3 increased after CRF treatment.

Furthermore, co-immunoprecipitation revealed an enhanced interaction between PDIA3 and STAT3 or p-STAT3 on the membranes of JAWSII cells after CRF treatment (Fig. 3B). As expected, these heightened interactions were further confirmed on the membranes of MNLDCs of IBS rats (Fig. 3C). Moreover, Fig. 3D demonstrates an increase in PDIA3 and p-STAT3 expression on the membrane and a
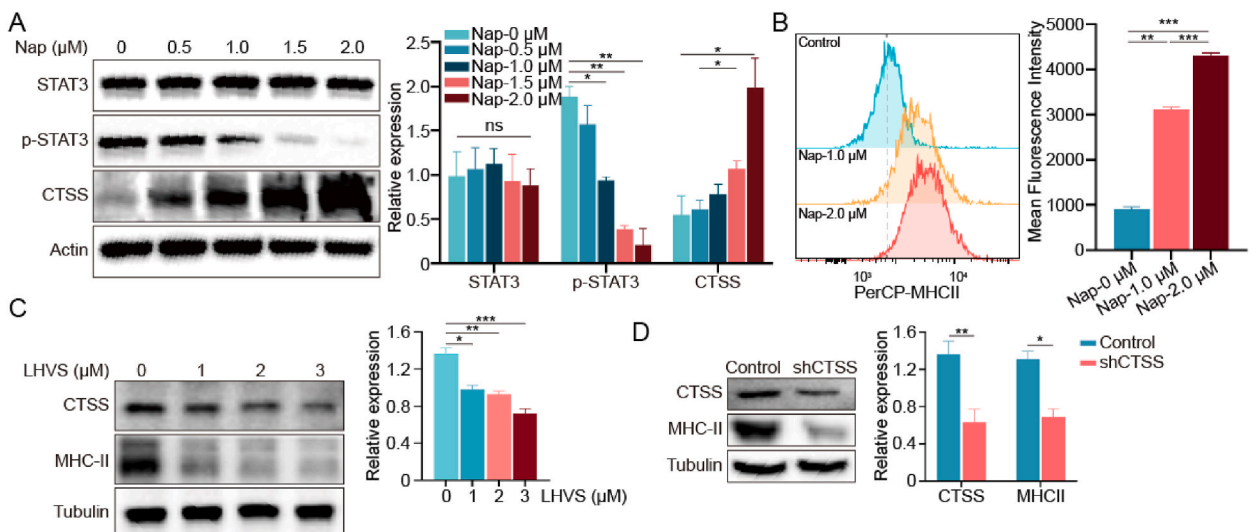

Fig. 4. (A, left) Immunoblot analysis of STAT3, p-STAT3, and CTSS proteins in JAWSII cells following Napabucasin treatment (p-STAT3 inhibitor) at various concentrations (0, 0.5, 1.0, 1.5, and 2 μM). (B) Flow cytometry results revealed an increase in surface MHC-II levels on JAWSII cells after exposure to Napabucasin (1 μM and 2 μM) compared to control cells. (C–D) The expression of CTSS and MHC-II following CTSS inhibition or knockdown. Values are presented as means ± SEM. "n.s." indicates no significance, *P < 0.05, **P < 0.01, ***P < 0.001.
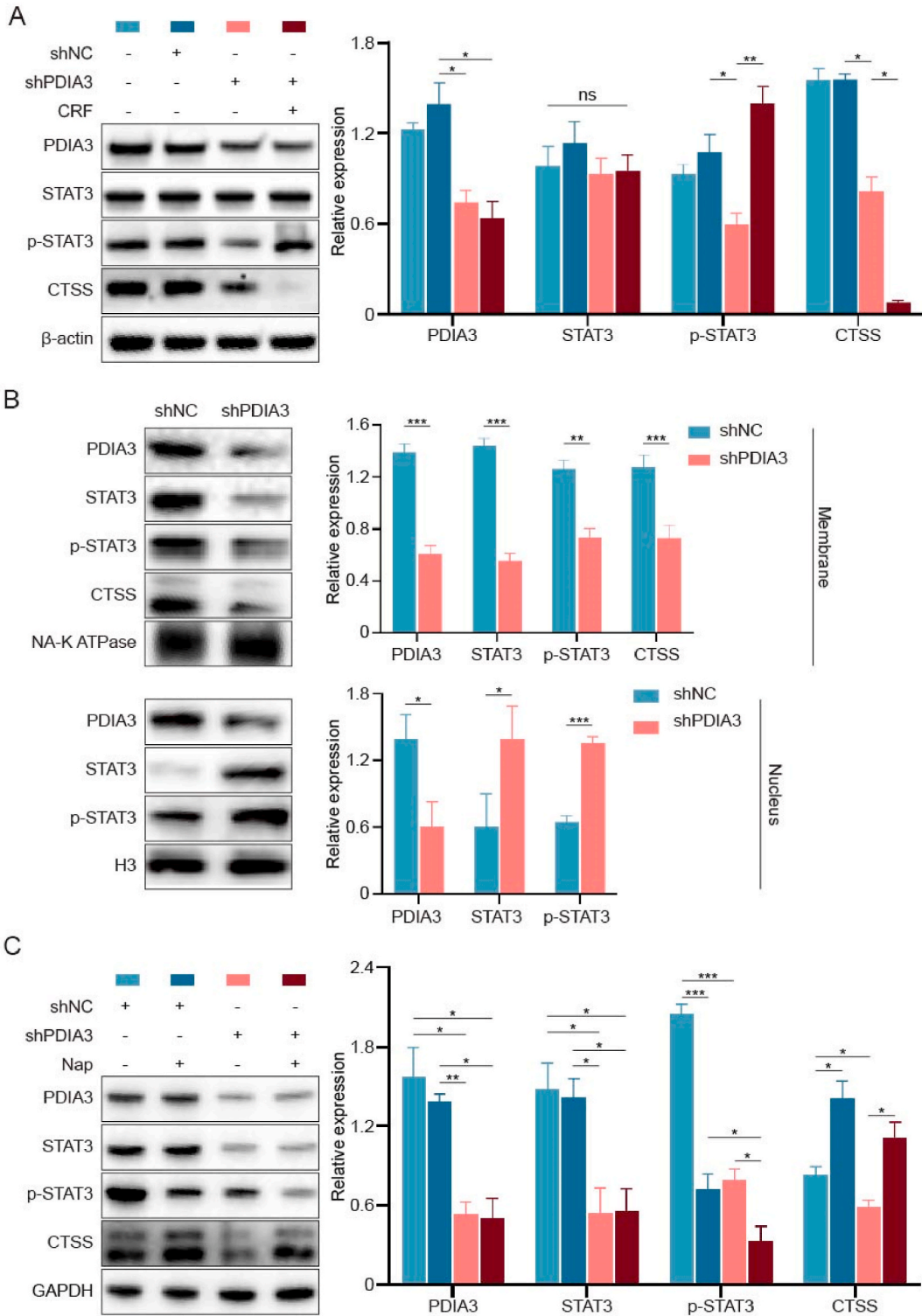
Fig. 5. The expression of correlated proteins in JAWSII cells with PDIA3 silencing. (A) JAWSII cells were transfected with Ctrl shNC, sh-PDIA3, and sh-PDIA3, respectively, and treated with CRF (100 nM, 24 h). (B) The expression of the collective proteins on the cell membrane and in the nucleus after PDIA3 silencing. (C) The effect of the p-STAT3 inhibitor in treating JAWSII cells after PDIA3 knockdown. All quantitative data are presented as means ± S.E.M. from three independent experiments. "n.s." represents no significance, *P < 0.05, **P < 0.01, ***P < 0.001. sh-NC, control shRNA; sh-PDIA3, PDIA3 shRNA.

decrease in the nucleus of DCs from IBS rats. These results underscore the upregulation of the interaction between PDIA3 and STAT3/p-STAT3 on the membrane of DCs in the IBS model. In addition, The expression of CTSS exhibited an increased tendency in the IBS group compared with the normal group, suggesting that membrane CTSS may play a crucial role in MHC-II activation (Fig. 3E).

2.4. p-STAT3/CTSS pathway was critical for MHC-II activation in DCs

To delve into the role of p-STAT3 and CTSS in MHC-II activation in DCs, we employed p-STAT3 inhibitor (Napabucasin) and CTSS inhibitor (LHVS) in JASWII cells. As shown in Fig. 4A, Napabucasin effectively reduced the expression of p-STAT3 in a dose-dependent manner. Additionally, CTSS levels increased in a dose-dependent fashion upon Napabucasin treatment (Fig. 4A). Correspondingly, Fig. 4B, using flow cytometry, illustrates an increase in MHC-II expression in JASWII cells following Napabucasin treatment. Furthermore, CTSS inhibition by LHVS significantly downregulated MHC-II expression, as confirmed by both Western blot and flow cytometry analyses (Fig. 4C and D). These findings underline the critical role of the p-STAT3/CTSS pathway in MHC-II activation in DCs.

2.5. PDIA3 was the key in p-STAT3/CTSS pathway in vitro

Previous findings suggested a potential mechanism in the DCs of IBS patients, indicating that PDIA3 could strongly interact with p-STAT3, thereby hindering the nuclear import of p-STAT3 and subsequently increasing the expression of CTSS and MHC-II. To further validate the role of PDIA3, we employed shRNA to selectively reduce PDIA3 expression in JAWSII cells. A simultaneous reduction in both p-STAT3 and CTSS was observed in JAWSII cells compared to the shNC group (Fig. 5A). Furthermore, CRF treatment restored p-STAT3 expression while further reducing CTSS expression (Fig. 5A). To elucidate this phenomenon, we conducted membrane and nucleus separation of JAWSII cells to assess the expression of relevant proteins. With PDIA3 knockdown, membrane p-STAT3 decreased, while nuclear p-STAT3 increased (Fig. 5B). Subsequently, we employed a p-STAT3 inhibitor to treat JASWII cells after PDIA3 knockdown. As expected, the p-STAT3 inhibitor successfully rescued CTSS expression (Fig. 5C). These results align with our hypothesis. Following PDIA3 knockdown, the weakened interaction of PDIA3 and p-STAT3 on the membrane increased the nuclear import of p-STAT3, even with a decreased total expression of p-STAT3, contributing to the downregulation of CTSS.

*2.6. PDIA3 of MLNDCs was the key target in the prevention and the treatment of IBS*

In the next phase, lentivirus was utilised to knockdown PDIA3 in rat MLNDCs. Specifically, we administered the lentivirus either after the induction of IBS in rats, representing preventive intervention ("shPDIA3 after"), or concurrently with the induction of IBS, representing therapeutic intervention ("shPDIA3 concurrent"). As depicted in Fig. 6A, PDIA3 knockdown effectively ameliorated abnormal stool characteristics and the AWR score in IBS rats, alleviating typical IBS symptoms. At the protein level, p-STAT3 (including p-STAT3/STAT3) and CTSS were reduced in the PDIA3 knockdown "after" and "concurrent" IBS groups compared with the IBS or vector virus IBS group (Fig. 6B). The expression of PDIA3, STAT3, p-STAT3, and CTSS on the membrane of DCs increased in the IBS or IBS vector virus group compared with the control group but decreased in the "after" and "concurrent" PDIA3 knockdown groups (Fig. 6C). Furthermore, the expression of STAT3 and p-STAT3 decreased in the IBS or IBS vector virus group in the nucleus of DCs compared with the control group but increased in the "after" and "concurrent" PDIA3 knockdown groups (Fig. 6D). Additionally, the interaction and co-localisation of PDIA3 with STAT3 or p-STAT3 on the membrane of DCs were reduced with PDIA3 knockdown (Fig. 6E and F). In summary, as a crucial upstream regulator of the p-STAT3/CTSS/MHC-II pathway, PDIA3 emerges as a promising target for preventing the onset of IBS and treating IBS patients.

2.7. Active DCs promote the proliferation of CD4$^+$ T cells in IBS model

Dysregulated immune cells, including CD4$^+$ T cells, secrete various cytokines that contribute to the development of IBS [21]. To investigate whether MLNDCs could influence the secretion of relevant cytokines, we conducted mixed leukocyte reactions. Co-culturing with MLNDCs from the IBS group resulted in a significant proliferation of CD4$^+$ T cells compared to the control group (Fig. 6G and H). Furthermore, the proliferation of CD4$^+$ T cells notably decreased after or concurrently with PDIA3 knockdown (Fig. 6G and H). Additionally, the MHC-II expression of MLNDCs exhibited a similar trend (Fig. 6I), indicating a potential connection between DCs and CD4$^+$ T cells. Notably, the co-cultured medium showed an elevation in IL-4, IL-6, IL-9, and TNF-α in the IBS rat group, whereas it decreased in the "after" or "concurrent" PDIA3 knockdown groups (Fig. 6J–M). These findings suggest that DC activation can stimulate CD4$^+$ T cell proliferation and enhance the production of relevant cytokines, contributing to immune system dysregulation and subsequently triggering the development of IBS.

2.8. Punicalagin could rescue the formation of IBS by inhibiting PDIA3 of MLNDCs

Pomegranate, a widely cultivated fruit with significant medicinal value, particularly in its peel, is known to contain active compounds. Among these compounds, punicalagin (Pun) stands out as a crucial component [22]. Pun is often hydrolyzed into ellagic acid and urolithins, imparting various biological antioxidative effects, including antitumor, antibacterial, and anti-inflammatory properties [23]. Additionally, Pun has been identified to bind to PDIA3 and inhibit its disulfide reductase activity [24]. To assess whether Pun could inhibit PDIA3 in MLNDCs, we treated JASWII cells with Pun. As depicted in Fig. 7A, Pun exhibited a dose-dependent inhibitory
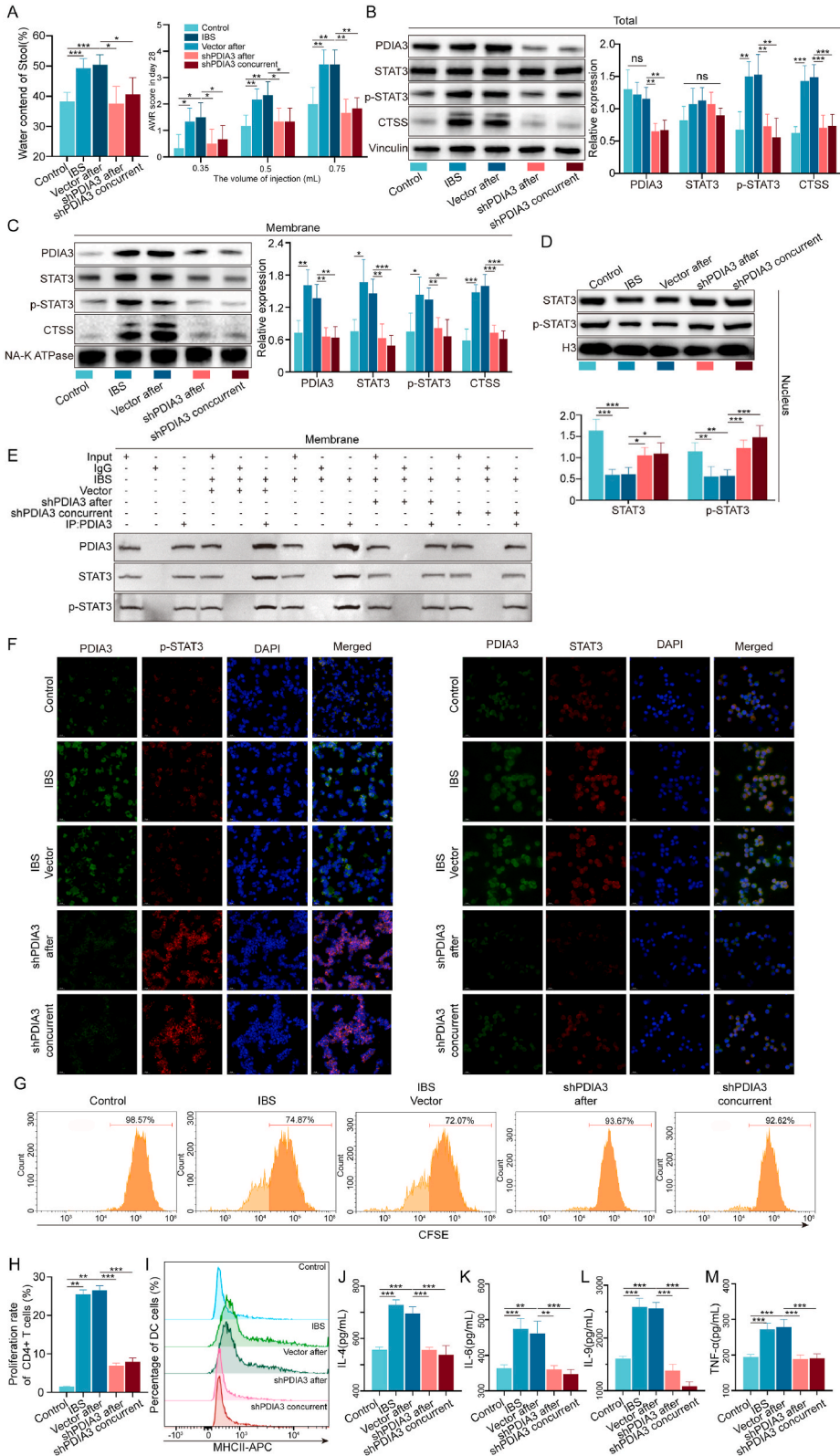
(caption on next page)

Fig. 6. The effect of PDIA3 knockdown in vivo (n = 6/group). (A) Water content of stool at day 14; AWR scores at pressure stimulations of 0.35 mL, 0.5 mL, and 0.75 mL. (B) The expression of correlated proteins in MLNDCs from five groups (Control, IBS, IBS + vector, sh PDIA3 after IBS construction, and sh PDIA3 concurrent IBS, respectively). (C–D) The expression of correlated proteins on the cell membrane and in the nucleus of MLNDCs from the five groups. (E) A co-immunoprecipitation experiment detected the association of PDIA3 with STAT3 and its phosphorylation on the cell membrane of MLNDCs. (F) Immunofluorescent staining of PDIA3 (green), STAT3/p-STAT3 (red), and the nucleus (DAPI, blue) (original magnification × 600) in the five groups. (G–H) MLNDCs (5 × 105) from the five groups were incubated for 5 days with increasing amounts of carboxyfluorescein diacetate succinimidyl ester (CFSE)-labelled T cells from the spleens of C57BL/6 mice. CFSE profiles of CD4$^+$ T cells are shown. (I) The MHC-II expression of MLNDCs was detected by flow cytometry in the five groups. (J–M) The co-cultured medium was tested for the levels of IL-4, IL-6, IL-9, and TNF-α in the five rat groups. Values represent means ± SEM. "n.s." indicates no significance, *$P < 0.05$, **$P < 0.01$, ***$P < 0.001$. (For interpretation of the references to color in this figure legend, the reader is referred to the Web version of this article.)

effect on PDIA3. Subsequently, a modelling and treatment strategy was implemented in mice, as outlined in Fig. 7B. The results indicated that Pun successfully inhibited PDIA3 expression in MLNDCs (Fig. 7C). Furthermore, the IBS model was successfully established by day 14, and Pun therapy effectively alleviated typical IBS symptoms (Fig. 7D–F). Moreover, HE staining images of various organs demonstrated similarity across different groups (Fig. 7G), suggesting that the drug had no significant toxicity on normal tissues, including the heart, liver, spleen, lung, kidney, and brain. In conclusion, Pun emerges as a potential therapeutic agent for alleviating IBS by inhibiting PDIA3 in MLNDCs.

3. Discussion

The global incidence of IBS is on the rise due to the increasing modernization of countries. The pathophysiology of IBS is intricate and multifactorial, involving factors such as genetics, diet, gut microbiota, gut endocrine cells, stress, and low-grade inflammation [10]. Recent investigations have underscored the significance of brain-gut axis dysfunction as a crucial pathogenetic mechanism in IBS [25]. Numerous studies, both in animals and in clinical settings, have provided evidence that the interaction between sex hormones, particularly estrogen, and the 5-hydroxytryptamine (5-HT) and CRF signalling systems can modulate brain-gut axis dysfunction in IBS, thereby contributing to visceral sensitivity [26,27]. Within stress-activated pathways, the CRF signalling system stands out as a key element in the biochemical mechanism through which the brain translates stimuli into an integrated physical response [28]. In the context of this study, we employed in vitro and in vivo IBS models to delve into the underlying mechanisms of IBS.

Various studies have associated PDIA3 with multiple diseases [29–34]. In a prior investigation, PDIA3 expression exhibited significant upregulation in a stress-related animal model, correlating positively with abnormal immune responses in CD4$^+$ T cells [12,35]. Additionally, existing literature indicates that PDIA3 in DCs is involved in these processes [35]. Moreover, prior evidence suggests that nuclear PDIA3 acts as a chaperone, interacting with DNA and enhancing DNA binding to the STAT3 complex, thereby facilitating proximal transcription factors. In the current study, we initially observed the co-localisation and interaction of PDIA3 and STAT3 on the membrane of DCs. Notably, upon PDIA3 silencing, a reduction in p-STAT3 protein levels was observed. This finding could be attributed to the absence of PDIA3 in the membrane complex, influencing the transcriptional potential of STAT3 and resulting in decreased p-STAT3 expression. Through cell-fractionation techniques, the study demonstrated alterations in the membrane expression levels of the PDIA3-STAT3 complex and certain relevant proteins in IBS. These outcomes suggest that the interaction of PDIA3-STAT3 on the membrane is a crucial response in IBS, potentially inducing the translocation of PDIA3 and p-STAT3 from the nucleus to the membrane. This study represents the first report highlighting the interaction of PDIA3 with STAT3 on the membrane of DCs in IBS.

Initial research suggested that PDIA3 is a chaperone for the endoplasmic reticulum [36]. Now, as vitamin D receptors, PDIA3 initiates membrane-associated cascade reactions [37–39]. Furthermore, it has been demonstrated that Vitamin D, as an immunoregulatory factor, plays a vital role in regulating intestinal homeostasis as well as influencing IBD progression [40]. A higher incidence of vitamin D insufficiency and deficiency has been observed in IBD patients [41], indicating that PDIA3 might play a role in this condition. We will focus on the relationship between PDIA3 and IBD in our upcoming study, which has been limited to date due to limited research.

According to Kwan et al., deletion of PDIA3 impacts mitochondrial morphology and bioenergetics, likely via STAT3 regulation, and affects mitochondrial response to 1,25(OH)2D3 [43]. As PDIA3 was found also in mitochondria [42], and we are concerned about the impact of the interaction between PDIA3 and STAT3 on IBS on the DC cell membrane, we cannot rule out direct effects on mitochondrial structure and function. Hence, this requires more experiments to prove.

STAT3 is a member of the STAT family, a group of signal-responsive transcription factors primarily regulated through phosphorylation [43]. The regulation of STAT3 involves two critical phosphorylation sites. Tyr705 phosphorylation, triggered by cytokine stimulation, is mediated by Janus kinases including Jak1, Jak2, and Tyk2, with Jak1 being the preferred kinase. By phosphorylating Tyr705, STAT3 homodimers, translocates to the nucleus, binds to DNA, and activates transcription [42]. Serine 727 (S727) is another STAT3 phosphorylation site [44]. The phosphorylation of Ser727 within the transactivation domain follows the phosphorylation of Tyr705 [45]. Further, mitochondrial function appears to be dependent on Ser-727 phosphorylation rather than Tyr-705 phosphorylation of STAT3. PDIA3 interacts with STAT3 [46] to regulate Tyr705 phosphorylation [47,48] and also suppresses Ser727 phosphorylation [49]. In our study, we indicated that PDIA3 interacts directly with STAT3 to suppress pY705 transfer to the nucleus IBS model, which results consist with previous studies [47,48]. By increasing the amount of p-STAT3 Y705 in the membrane, CTSS is activated, promoting the formation of IBS inflammatory factors. CTSS plays a pivotal role as a lysosomal cysteine protease and is physiologically essential in professional antigen-presenting cells, including macrophages, dendritic cells (DCs), and B cells [21]. It primarily governs MHC-II-related antigen presentation [50]. The activity of CTSS, mediated by STAT3, influences MHC-II ab dimer
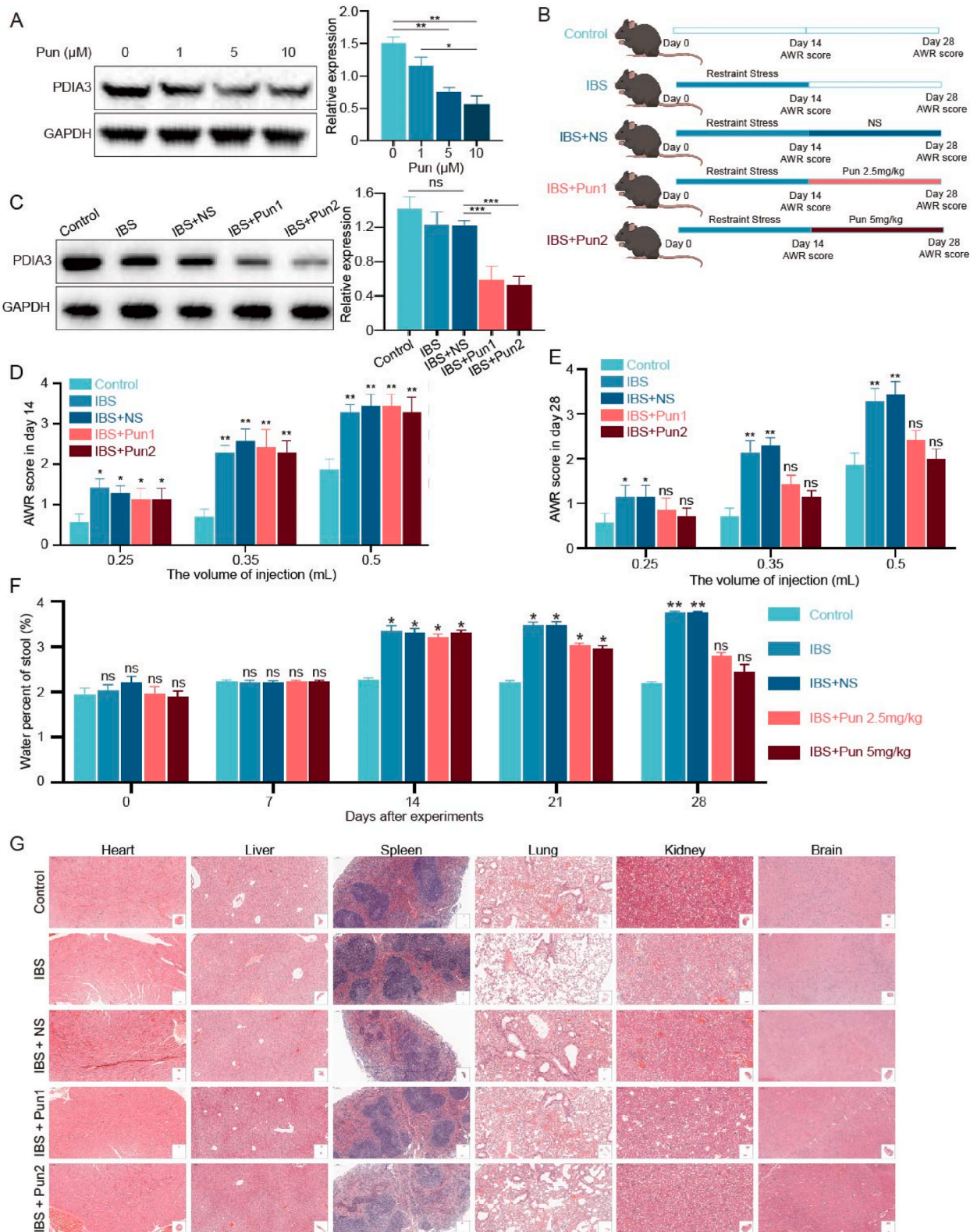
(caption on next page)

Fig. 7. The effect of Punicalagin (Pun) in IBS (n = 6/group). (A and C) The expression of PDIA3 in DCs after Pun treatment in vitro and in vivo, respectively. (B) Schematic illustrations of experimental protocols. The intervention timeline for the control group, IBS group, IBS + NS group, IBS + Pun group (2.5 mg/kg), and IBS + Pun group (5 mg/kg). (D–F) AWR scores at pressure stimulations of 0.25 mL, 0.35 mL, and 0.5 mL on days 14 and 28; Water percentage in the stool of mice on days 0, 7, 14, 21, and 28. (G) Representative H&E staining images of various organs after NS or Pun treatment. Values represent means ± SEM. "n.s." indicates no significance, *$P < 0.05$, **$P < 0.01$, ***$P < 0.001$. NS, Normal saline; H&E, hematoxylin and eosin.

levels in DCs, as well as CD4$^+$ T cell-mediated immunity [19]. In this study, a molecular inhibitor of p-STAT3 was employed to assess the potential of p-STAT3 in negatively regulating CTSS. This aligns with a prior study demonstrating that CTSS upregulation is impeded by STAT3 activation [43]. These findings suggest that STAT3-mediated CTSS activity could enhance the expression levels of the surface marker MHC-II. This, in turn, might induce the proliferation of CD4$^+$ T cells, leading to the secretion of various cytokines in conjunction with CD4$^+$ T cells, thereby mediating the immune function of DCs.

Several studies report increased T cell numbers in different intestinal mucosal compartments, implicating an activated adaptive immune response in IBS pathogenesis. Notably, elevated CD4$^+$ T cell levels have been consistently observed in the colons of IBS patients [51–53], and mucosal mast cell numbers are consistently augmented in both the small and large intestines [52,54–56]. Our previous work demonstrated that CRF enhances the ability of MLNDCs to stimulate CD4$^+$ T lymphocytes, leading to increased IL-4 and IL-9 secretion and mast cell induction [9,57]. In the current study, co-culturing with the MLNDCs from the IBS model resulted in significant CD4$^+$ T cell proliferation. This may be linked to their functional and developmental processes, as CD4$^+$ T cells play a crucial role in regulating immune responses and maintaining immune homeostasis [45]. Additionally, they actively participate in immune processes against exogenous antigens by enhancing the binding of the T cell receptor (TCR) to the antigen-MHC Class II molecular complex [58].

Treatment strategies for IBS patients encompass dietary, psychotherapeutic, pharmacotherapeutic, and microbial approaches [4]. Recent evidence highlights the effectiveness of various plant-derived natural products, such as terpenoids, flavonoids, alkaloids, and phenols, in managing IBS. These natural products demonstrate positive effects by alleviating depression, anxiety, visceral hypersensitivity, and intestinal permeability. Molecular mechanisms involve enhancing the expression of tight junctions and mucus proteins, modulating the brain-gut axis and gut microbiota structure, elevating short-chain fatty acid levels, inhibiting the **NF-κB/MLCK** signaling pathway, thereby attenuating inflammatory reactions and mitigating intestinal mucosal damage [59]. In our study, Pun administration significantly improved intestinal sensitivity in mice, reducing thresholds for abdominal lifting and back arching, and increasing mouse weight. This underscores the beneficial role of Pun in addressing visceral hypersensitivity in IBS. However, the
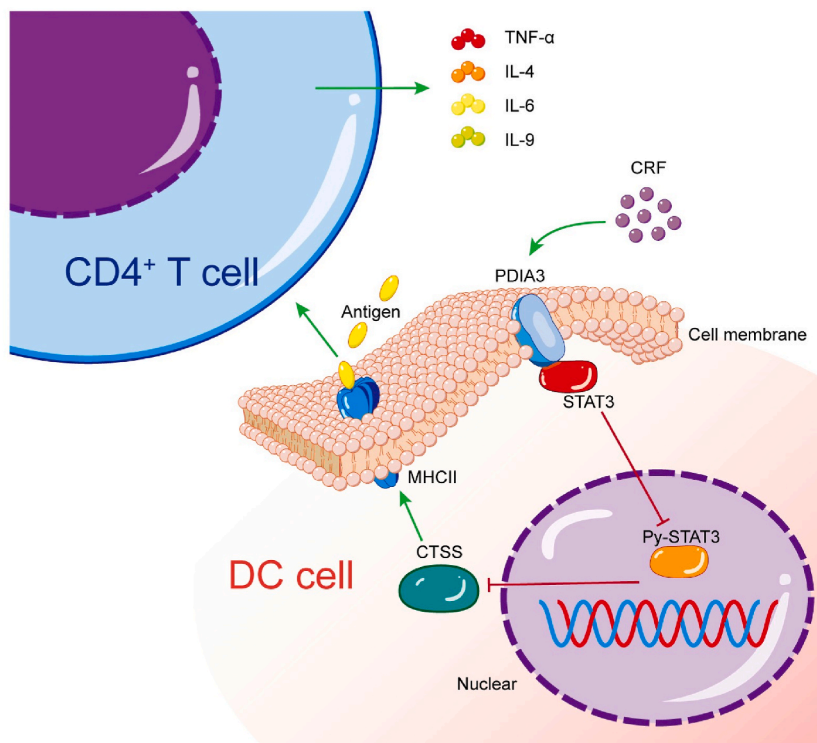

Fig. 8. Flow diagram illustrating the mechanisms of stress-related immune abnormalities in IBS. In IBS, the formation of the PDIA3-STAT3 protein complex in MLNDCs inhibits the translocation of p-STAT3 into the nucleus. This leads to an upregulation of CTSS and MHC-II protein expression, subsequently triggering the immune and inflammatory response.

molecular mechanisms remain unclear and warrant further investigation.

This study reveals a novel interaction between PDIA3 and STAT3 on the membrane of MLNDCs, which hinders the STAT3-DNA binding process and subsequently upregulates the CTSS/MHC-II signalling pathway. The observed association between PDIA3 and STAT3 in the IBS model, as confirmed by the regulation of STAT3's transcriptional potential (Fig. 8), provides fresh insights into the modulation of immune and inflammatory reactions. Further exploration of the function and mechanisms of PDIA3 compounds holds the promise of unveiling new therapeutic strategies and targets, thereby paving the way for innovative IBS treatments in the future.

4. Methods

We procured the following reagents and materials for this study: Minimum Essential Medium (MEM)-alpha, Foetal Bovine Serum (FBS), L-Glutamine, and trypsin from Gibco (USA); Granulocyte-Macrophage Colony-Stimulating Factor (GM-CSF) from Peprotech (USA); Corticotropin-Releasing Factor (CRF) from Tocris Bioscience (UK); PVDF membranes from Millipore (USA); Protein A/G from Bimake (USA); RNeasy Mini Kit from OMEGA (China); Reverse Transcription Kit and PCR TliRNaseH Plus from Tiangen Technology (China); Minute™ Plasma Membrane Protein Isolation and Cell Fractionation Kits from Invent Biotechnologies (China); Protein A/G Magnetic Beads (Bimake); and p-STAT3 inhibitor from Selleck.

4.1. JAWSII cell culture

JAWSII cells, sourced from the American Type Culture Collection (ATCC), were cultivated in MEM-alpha medium supplemented with 20 % v/v Foetal Bovine Serum (FBS), 5 ng/ml Granulocyte-Macrophage Colony-Stimulating Factor (GM-CSF), and 4 mM L-glutamine. Culturing was conducted in a humidified atmosphere with 5 % CO_2 at 37 °C. JAWSII cells are immortal immature dendritic cell lines derived from mouse bone marrow culture. They exhibit characteristics akin to colonic dendritic cells, including maturation and activation markers, and can induce an immune response resembling dendritic cells. To obtain both adherent and non-adherent cells, semi-adherent JAWSII cells were separated via centrifugation and trypsinization.

4.2. Experimental animals

Male Sprague-Dawley (SD) rat weighing between 200 and 250 g (mice, 20-25g) were housed under controlled conditions with a temperature of 22 ± 1 °C, humidity maintained at 65–70 %, and subjected to a 12-h light/dark cycle. These rats and mice were kept at the Animal Center of Zhejiang Chinese Medical University in Hangzhou, China, with access to food and water ad libitum. All experimental procedures adhered to the guidelines set by the State Authority for Animal Research Conduct.

4.3. IBS animal modelling method

Four groups were established: the control group, IBS group, IBS empty virus group, and IBS knockdown group. The control group received no treatment. In the IBS group, **normal rats** were separated from their mother for 3 h each morning (8:00–11:00) from the second day after birth for 14 days. The IBS empty virus group involved intravenous injection of empty virus in the neonatal rats. In the IBS knockdown group, normal rats were treated with intravenous injection of PDIA3 knockout virus during the neonatal period or following the successful establishment of IBS.

4.4. AWR measurement

A distension balloon catheter with an 8-Fr size and 2 mm external diameter was inserted into the descending colons of the rats and mice. Each distension period lasted 10 s and was followed by a 20-s resting period. The rats and mice experienced different levels of distension (0, 0.2, 0.3, and 0.4 mL) twice. After each measurement, the balloon was deflated and removed. Visceral sensory responses to colorectal distension (CRD) were quantified by assigning AWR scores as follows: 0 for no behavioural response, 1 for a brief head movement followed by immobility, 2 for abdominal muscle contraction, 3 for lifting of the abdomen, and 4 for body arching and lifting of the pelvic structures [60].

4.5. Isolation of mesenteric lymph node dendritic cells

The rats were euthanized by cervical dislocation, and mesenteric lymph nodes near the ileocecal junction were aseptically excised. These tissue samples were submerged in 5 mL of RPMI1640 (Gibco) and gently agitated between frosted glass slides. The resultant tissue preparations were passed through a 200 μm cell filter to obtain single-cell suspensions. The cells underwent two rounds of centrifugation at 200*g* for 10 min each. Dendritic cells (DCs) were subsequently incubated with a mixture containing OX62 microbeads (Miltenyi Biotec, Bergisch Gladbach, Germany), FcR blocking reagent (Miltenyi Biotec), and buffer in a 1:1:3 ratio for 15 min at 4 °C. Following incubation, DC populations were enriched through magnetic bead sorting using MACS columns (Miltenyi Biotec). This sorting process was repeated to enhance the purity of DCs. The purity of dendritic cells, based on the surface phenotype of the isolated cells, was determined through flow cytometric analysis using the FACSCantoII system (BD Biosciences, San Jose, USA), which typically resulted in a high level of purity following magnetic sorting.

4.6. Immunoblot analysis

The primary antibodies detected by Western blot are shown in Table 1. Cell lysis was performed with chilled RIPA buffer (P0013B; Beyotime) at 4 °C for 30 min. Equal quantities of total protein were separated via 10 % sodium dodecyl sulphate-polyacrylamide gel electrophoresis (SDS-PAGE) and then transferred to nitrocellulose membranes (Life Sciences). These membranes were blocked with 5 % non-fat milk in TBST for 1 h, followed by an overnight incubation with the respective primary antibodies at 4 °C. After three washes with TBST, the membranes were exposed to HRP-linked secondary antibodies for 1 h. Detection was carried out using the ECL kit (SQ201; Epizime Biotechnologies). Cell fractionation into membrane and nuclear fractions was performed using the Minute™ plasma membrane protein isolation and cell fractionation kit (#SM005; Invent Biotechnologies) following the manufacturer's instructions. The resulting fractions were analysed through SDS-PAGE and western blotting with specific antibodies. For quantification of the immunoreactive bands, Quantity One (Bio-Rad) was utilised.

4.7. Immunofluorescence staining

JAWSII cells were cultured on chamber slides at a concentration of 10ˆ5 cells per millilitre. After aspirating the medium, the cells were air-dried and fixed with 4 % formalin for 10 min at 25 °C. Subsequently, the cells were blocked for 30 min, followed by incubation with anti-PDIA3 rabbit (1:200) and anti-STAT3 mouse (1:200) antibodies in a humid chamber at 4 °C overnight. Further incubation was carried out with AF488-conjugated anti-rabbit and CY3-conjugated anti-mouse secondary antibodies (both at 1:400) for 1 h in the dark. DAPI counterstaining was performed for 15 min as an anti-quencher. Image acquisition was performed using a laser confocal microscope (Leica, Germany), BD Pathway 435 High Content Bioimagers (BD Biosciences, USA), and Nikon Intensilight C-HGFI Fiber Illuminator (Nikon Corporation, Japan). Image analysis was conducted using COMOS (Siemens, USA).

4.8. Co-immunoprecipitation

To extract total protein, wells containing over 1×10^7 cells upon seeding were used. Cell lysis was performed using chilled Pierce™ IP Lysis Buffer (Thermo Fisher Scientific), supplemented with protease inhibitor (P8340; CST) for 10 min. After centrifugation (14,000g for 10 min at 4 °C), the collected supernatants were further analysed. The lysates were subjected to co-immunoprecipitation using anti-IgG (1:50), anti-ERp57 (1:50), or anti-STAT3 (1:50) for 1 h at 37 °C. The cell lysate, antibodies, and protein A/G Magnetic Beads (25–50 μl) were co-incubated overnight at 4 °C. Subsequently, the samples were centrifuged (12,000 g for 30 s at 4 °C), and the complexes were subjected to four washes with immunoprecipitation buffer. Bound proteins were identified through immunoblot analysis. Normal mouse or rabbit IgG (1:50) was employed as a negative control.

4.9. Cell and animal transfection

Short hairpin RNAs (shRNAs) were provided by Taitool Biocscience (China). PDIA3 shRNA was denoted as Lentai-hU6-shRNA-PDIA3 (cat. no. WL1059; ACCGGGCAACTTGAGAGATAACTATTCAAGAGATAGTTATCTCTCAAGTTGCTTTT); scramble shRNA (cat. no. L7012) served as the negative control. Both shRNAs were used at a MOI of 50. Fresh medium was added 24 h following cell seeding, and the cells were cultured in the normal culture medium 12 h after transfection. Quantitative real-time polymerase chain reaction (qRT-PCR) and immunoblot analyses were conducted to assess transfection efficiency.

We designed the three sgRNA target sequences using the online tool CRISPR-ERA (http://crispr-era.stanford.edu/index.jsp). Three target sequences that each had high similarity with both PDIA3 genes, and few putative off-target sites were selected as candidate sgRNAs (Supplement Fig.1A). The three sgRNA sequences were cloned into pHBAAV-CMV-Sacas9-U6-gRNA vector to complete the constructs (Hanbio, cat. AAV023, Supplement Fig. 1B) according to published protocols [DOI: 10.1089/hum.2008.188]. Sequencing confirmed that the PCR product of r-Pdia3-gRNA1 had a slight target effect, while r-Pdia3-gRNA2/3 had no target effect (Supplement Fig. 1C and 1D).

Table 1
Primary antibodies for western blotting.

Protein	Manufacturer	Cat.#
PDIA3	Proteintech	15967-1-AP
STAT3	CST	12640S
STAT3	CST	9139S
p-STAT3(Tyr705)	CST	4113S
p-STAT3(Tyr705)	CST	9145S
Na-K ATPase	Abbkine	ABP51894
H3	CST	4499S
IgG	CST	2729
CTSS	Santa Cruz Biotechnology	4499S
CTSS	Huabio	HA500422
MHC-II	absin	abs127651
β-actin	CST	3700S

4.10. Flow cytometry

JAWSII cells were seeded in 96-well plates at a density of 105 cells/well and were incubated with the STAT3 inhibitor for 24 h. Following this incubation, cell surface markers were analysed using flow cytometry. In brief, the cells were incubated with MHC-II/FITC and FITC-mouse IgG2b control antibodies according to the manufacturer's instructions for 30 min at 4 °C. Fluorescence was detected on a FACS Calibur, and data analysis was performed using FACSDIVA (BD Biosciences).

4.11. Mixed leukocyte reactions

JAWSII cells were cultured in 96-well plates (5×10^5 cells per well) and treated with OVA (100 nM) for 24 h. Splenocytes from male C57BL/6 mice, labelled with carboxyfluorescein diacetate succinimide (CFSE), were used to assess T cell proliferation [61]. Equal amounts of CFSE-labelled lymphocytes were added to each well for a 5-day incubation in RPMI 1640 containing penicillin (100 U/ml), L-glutamine (2 mM), heat-inactivated fetal calf serum (10 %), and streptomycin (100 μg/ml). Subsequently, the cells were stained with anti-rat CD4 antibodies. Flow cytometry was used to examine the amounts of CFSE-labelled $CD4^+$ T cells.

4.12. Statistical analysis

The data are presented as mean ± standard error of the mean (SEM) or standard deviation (SD) and were compared using one-way analysis of variance (ANOVA) or the independent samples *t*-test. A p-value of less than 0.05 indicated statistical significance. SPSS 20.0 (SPSS, USA) and GraphPad Prism v6.0 (GraphPad Software, USA) were utilised for data analysis.

Funding statement

Data availability statement

Data will be made available on request.

Ethics statement

The investigation adhered to the Experimental Animal Administration regulations promulgated by the State Committee of Science and Technology of the People's Republic of China. The present study was approved by the Laboratory animal management and ethics committee of Zhejiang Chinese Medical University. (Approval No. IACUC-20211011-02). All the procedures for the care of the rats were in accordance with the institutional guidelines for animal use in research.

CRediT authorship contribution statement

Chunyan Weng: Writing – review & editing, Writing – original draft, Formal analysis. **Jingli Xu:** Writing – review & editing, Writing – original draft, Formal analysis. **Xiao Ying:** Formal analysis. **Shaopeng Sun:** Data curation. **Yue Hu:** Data curation. **Xi Wang:** Writing – review & editing, Funding acquisition. **Chenghai He:** Software. **Bin Lu:** Project administration, Funding acquisition. **Meng Li:** Project administration, Funding acquisition.

Declaration of competing interest

The authors declare that they have no known competing financial interests or personal relationships that could have appeared to influence the work reported in this paper.

References

[1] D.A. Drossman, L. Chang, W.D. Chey, et al., Rome IV: Functional Gastrointestinal Disorders/Disorders of Gut-Brain Interaction [M], fourth ed., The Rome foundation, 2016. Raleigh, NC.
[2] B.E. Lacy, F. Mearin, L. Chang, W.D. Chey, A.J. Lembo, M. Simren, et al., Bowel disorders, Gastroenterology 150 (2016) 1393–1407, https://doi.org/10.1053/j.gastro.2016.02.031.
[3] M.G. Shiha, I. Aziz, Review article: physical and psychological comorbidities associated with irritable bowel syndrome, Alimentary pharmacology & therapeutics 54 (Suppl 1) (2021) S12–s23, https://doi.org/10.1111/apt.16589.
[4] M. Camilleri, Diagnosis and treatment of irritable bowel syndrome: a review, JAMA 325 (2021) 865–877, https://doi.org/10.1001/jama.2020.22532.
[5] B.D. Naliboff, et al., Mindfulness-based stress reduction improves irritable bowel syndrome (IBS) symptoms via specific aspects of mindfulness, Neuro Gastroenterol. Motil. : the official journal of the European Gastrointestinal Motility Society 32 (2020) e13828, https://doi.org/10.1111/nmo.13828.
[6] Y. Long, et al., Characteristics of intestinal lamina propria dendritic cells in a mouse model of postinfectious irritable bowel syndrome, J. Gastroenterol. Hepatol. 27 (2012) 935–944, https://doi.org/10.1111/j.1440-1746.2011.07046.x.

[7] M. Li, et al., Role of dendritic cell-mediated abnormal immune response in visceral hypersensitivity, Int. J. Clin. Exp. Med. 8 (2015) 13243–13250.
[8] Q. Zhao, et al., Clostridium butyricum alleviates intestinal low-grade inflammation in TNBS-induced irritable bowel syndrome in mice by regulating functional status of lamina propria dendritic cells, World J. Gastroenterol. 25 (2019) 5469–5482, https://doi.org/10.3748/wjg.v25.i36.5469.
[9] L. Meng, et al., Corticotropin-releasing factor changes the phenotype and function of dendritic cells in mouse mesenteric lymph nodes, Journal of neurogastroenterology and motility 21 (2015) 571–580, https://doi.org/10.5056/jnm15019.
[10] J. Aguilera-Lizarraga, H. Hussein, G.E. Boeckxstaens, Immune activation in irritable bowel syndrome: what is the evidence? Nat. Rev. Immunol. 22 (2022) 674–686, https://doi.org/10.1038/s41577-022-00700-9.
[11] M. Chiavari, et al., PDIA3 expression in glioblastoma modulates macrophage/microglia pro-tumor activation, Int. J. Mol. Sci. 21 (2020), https://doi.org/10.3390/ijms21218214.
[12] Y. Ding, et al., Proteomic analysis of colonic mucosa in a rat model of irritable bowel syndrome, Proteomics 10 (2010) 2620–2630, https://doi.org/10.1002/pmic.200900572.
[13] H.S. Li, S.S. Watowich, Diversification of dendritic cell subsets: emerging roles for STAT proteins, JAK-STAT 2 (2013) e25112, https://doi.org/10.4161/jkst.25112.
[14] P.B. Sehgal, Plasma membrane rafts and chaperones in cytokine/STAT signaling, Acta Biochim. Pol. 50 (2003) 583–594.
[15] P.B. Sehgal, G.G. Guo, M. Shah, V. Kumar, K. Patel, Cytokine signaling: STATS in plasma membrane rafts, J. Biol. Chem. 277 (2002) 12067–12074, https://doi.org/10.1074/jbc.M200018200.
[16] Y. Hu, et al., Corticotropin-releasing factor augments LPS-induced immune/inflammatory responses in JAWSII cells, Immunol. Res. 64 (2016) 540–547, https://doi.org/10.1007/s12026-015-8740-3.
[17] H. Kitamura, et al., IL-6-STAT3 controls intracellular MHC class II alphabeta dimer level through cathepsin S activity in dendritic cells, Immunity 23 (2005) 491–502, https://doi.org/10.1016/j.immuni.2005.09.010.
[18] J. Sage, et al., Modulation of the expression and activity of cathepsin S in reconstructed human skin by neohesperidin dihydrochalcone, Matrix Biol. : journal of the International Society for Matrix Biology 107 (2022) 97–112, https://doi.org/10.1016/j.matbio.2022.02.003.
[19] L.L. Chan, B.K. Cheung, J.C. Li, A.S. Lau, A role for STAT3 and cathepsin S in IL-10 down-regulation of IFN-gamma-induced MHC class II molecule on primary human blood macrophages, J. Leukoc. Biol. 88 (2010) 303–311, https://doi.org/10.1189/jlb.1009659.
[20] K.B. Hong, H. Seo, J.S. Lee, Y. Park, Effects of probiotic supplementation on post-infectious irritable bowel syndrome in rodent model, BMC Compl. Alternative Med. 19 (2019) 195, https://doi.org/10.1186/s12906-019-2610-9.
[21] Y. Nasser, et al., Activation of peripheral blood CD4+ T-cells in IBS is not associated with gastrointestinal or psychological symptoms, Sci. Rep. 9 (2019) 3710, https://doi.org/10.1038/s41598-019-40124-5.
[22] G. Ge, et al., Punicalagin ameliorates collagen-induced arthritis by downregulating M1 macrophage and pyroptosis via NF-κB signaling pathway, Sci. China Life Sci. 65 (2022) 588–603, https://doi.org/10.1007/s11427-020-1939-1.
[23] D. Atrahimovich, A.O. Samson, A. Khattib, J. Vaya, S. Khatib, Punicalagin decreases serum glucose levels and increases PON1 activity and HDL anti-inflammatory values in balb/c mice fed a high-fat diet, Oxid. Med. Cell. Longev. 2018 (2018) 2673076, https://doi.org/10.1155/2018/2673076.
[24] F. Giamogante, et al., Punicalagin, an active pomegranate component, is a new inhibitor of PDIA3 reductase activity, Biochimie 147 (2018) 122–129, https://doi.org/10.1016/j.biochi.2018.01.008.
[25] D.A. Drossman, Functional gastrointestinal disorders: history, pathophysiology, clinical features and Rome IV, Gastroenterology 150 (2016) 1262–1279.
[26] L. Lin, et al., Acute stress disrupts intestinal homeostasis via GDNF-RET, Cell Prolif. 53 (2020) e12889, https://doi.org/10.1111/cpr.12889.
[27] X. Li, et al., Costunolide ameliorates intestinal dysfunction and depressive behaviour in mice with stress-induced irritable bowel syndrome via colonic mast cell activation and central 5-hydroxytryptamine metabolism, Food Funct. 12 (2021) 4142–4151, https://doi.org/10.1039/d0fo03340e.
[28] H.Y. Qin, C.W. Cheng, X.D. Tang, Z.X. Bian, Impact of psychological stress on irritable bowel syndrome, World J. Gastroenterol. 20 (2014) 14126–14131, https://doi.org/10.3748/wjg.v20.i39.14126.
[29] C. Tohda, T. Urano, M. Umezaki, I. Nemere, T. Kuboyama, Diosgenin is an exogenous activator of 1,25D₃-MARRS/Pdia3/ERp57 and improves Alzheimer's disease pathologies in 5XFAD mice, Sci. Rep. 2 (2012) 535, https://doi.org/10.1038/srep00535.
[30] A.M. Vitello, Y. Du, P.M. Buttrick, L.A. Walker, Serendipitous discovery of a novel protein signaling mechanism in heart failure, Biochemical and biophysical research communications 421 (2012) 431–435, https://doi.org/10.1016/j.bbrc.2012.03.124.
[31] B. Furie, R. Flaumenhaft, Thiol isomerases in thrombus formation, Circ. Res. 114 (2014) 1162–1173, https://doi.org/10.1161/circresaha.114.301808.
[32] Y. Wu, et al., The disulfide isomerase ERp57 mediates platelet aggregation, hemostasis, and thrombosis, Blood 119 (2012) 1737–1746, https://doi.org/10.1182/blood-2011-06-360685.
[33] A. Hettinghouse, R. Liu, C.J. Liu, Multifunctional molecule ERp57: from cancer to neurodegenerative diseases, Pharmacology & therapeutics 181 (2018) 34–48, https://doi.org/10.1016/j.pharmthera.2017.07.011.
[34] D. Song, et al., Insights into the role of ERp57 in cancer, J. Cancer 12 (2021) 2456–2464, https://doi.org/10.7150/jca.48707.
[35] Z. Zhuang, L. Zhang, X. Wang, L. Tao, B. Lv, PDIA3 gene induces visceral hypersensitivity in rats with irritable bowel syndrome through the dendritic cell-mediated activation of T cells, PeerJ 4 (2016) e2644, https://doi.org/10.7717/peerj.2644.
[36] C. Turano, E. Gaucci, C. Grillo, S. Chichiarelli, ERp57/GRP58: a protein with multiple functions, Cellular & molecular biology letters 16 (2011) 539–563, https://doi.org/10.2478/s11658-011-0022-z.
[37] M.A. Żmijewski, Nongenomic activities of vitamin D, Nutrients 14 (2022), https://doi.org/10.3390/nu14235104.
[38] J. Chen, et al., Protein-disulfide isomerase-associated 3 (Pdia3) mediates the membrane response to 1,25-dihydroxyvitamin D3 in osteoblasts, J. Biol. Chem. 285 (2010) 37041–37050, https://doi.org/10.1074/jbc.M110.157115.
[39] I. Nemere, N. Garbi, G.J. Hämmerling, R.C. Khanal, Intestinal cell calcium uptake and the targeted knockout of the 1,25D3-MARRS (membrane-associated, rapid response steroid-binding) receptor/PDIA3/Erp57, J. Biol. Chem. 285 (2010) 31859–31866, https://doi.org/10.1074/jbc.M110.116954.
[40] F. Vernia, et al., Vitamin D in inflammatory bowel diseases. Mechanisms of action and therapeutic implications, Nutrients 14 (2022), https://doi.org/10.3390/nu14020269.
[41] A. Topalova-Dimitrova, I.V. Dimitrov, R. Nikolov, Lower vitamin D levels are associated with the pathogenesis of inflammatory bowel diseases, Medicine 102 (2023) e35505, https://doi.org/10.1097/md.0000000000035505.
[42] M.P. Keasey, et al., PDIA3 inhibits mitochondrial respiratory function in brain endothelial cells and C. elegans through STAT3 signaling and decreases survival after OGD, Cell Commun. Signal. : CCS 19 (2021) 119, https://doi.org/10.1186/s12964-021-00794-z.
[43] H.Y. Kwan, et al., Signal transducer and activator of transcription-3 drives the high-fat diet-associated prostate cancer growth, Cell Death Dis. 10 (2019) 637, https://doi.org/10.1038/s41419-019-1842-4.
[44] R. Yang, M. Rincon, Mitochondrial Stat3, the need for design thinking, Int. J. Biol. Sci. 12 (2016) 532–544, https://doi.org/10.7150/ijbs.15153.
[45] T. Decker, P. Kovarik, Serine phosphorylation of STATs, Oncogene 19 (2000) 2628–2637, https://doi.org/10.1038/sj.onc.1203481.
[46] H. Coe, J. Jung, J. Groenendyk, D. Prins, M. Michalak, ERp57 modulates STAT3 signaling from the lumen of the endoplasmic reticulum, J. Biol. Chem. 285 (2010) 6725–6738, https://doi.org/10.1074/jbc.M109.054015.
[47] R. Kondo, et al., Downregulation of protein disulfide-isomerase A3 expression inhibits cell proliferation and induces apoptosis through STAT3 signaling in hepatocellular carcinoma, Int. J. Oncol. 54 (2019) 1409–1421, https://doi.org/10.3892/ijo.2019.4710.
[48] W. Hu, et al., Vitamin D3 activates the autolysosomal degradation function against Helicobacter pylori through the PDIA3 receptor in gastric epithelial cells, Autophagy 15 (2019) 707–725, https://doi.org/10.1080/15548627.2018.1557835.
[49] J.G. Burniston, et al., Conditional independence mapping of DIGE data reveals PDIA3 protein species as key nodes associated with muscle aerobic capacity, J. Proteomics 106 (2014) 230–245, https://doi.org/10.1016/j.jprot.2014.04.015.

[50] Z. Meng, W. Klinngam, M.C. Edman, S.F. Hamm-Alvarez, Interferon-γ treatment in vitro elicits some of the changes in cathepsin S and antigen presentation characteristic of lacrimal glands and corneas from the NOD mouse model of Sjögren's Syndrome, PLoS One 12 (2017) e0184781, https://doi.org/10.1371/journal.pone.0184781.

[51] R.C. Spiller, et al., Increased rectal mucosal enteroendocrine cells, T lymphocytes, and increased gut permeability following acute Campylobacter enteritis and in post-dysenteric irritable bowel syndrome, Gut 47 (2000) 804–811, https://doi.org/10.1136/gut.47.6.804.

[52] C. Cremon, et al., Mucosal immune activation in irritable bowel syndrome: gender-dependence and association with digestive symptoms, Am. J. Gastroenterol. 104 (2009) 392–400, https://doi.org/10.1038/ajg.2008.94.

[53] V.S. Chadwick, et al., Activation of the mucosal immune system in irritable bowel syndrome, Gastroenterology 122 (2002) 1778–1783, https://doi.org/10.1053/gast.2002.33579.

[54] M. Guilarte, et al., Diarrhoea-predominant IBS patients show mast cell activation and hyperplasia in the jejunum, Gut 56 (2007) 203–209, https://doi.org/10.1136/gut.2006.100594.

[55] M.M. Walker, et al., Duodenal mastocytosis, eosinophilia and intraepithelial lymphocytosis as possible disease markers in the irritable bowel syndrome and functional dyspepsia, Alimentary pharmacology & therapeutics 29 (2009) 765–773, https://doi.org/10.1111/j.1365-2036.2009.03937.x.

[56] A. Akbar, et al., Increased capsaicin receptor TRPV1-expressing sensory fibres in irritable bowel syndrome and their correlation with abdominal pain, Gut 57 (2008) 923–929, https://doi.org/10.1136/gut.2007.138982.

[57] Z.M. Zhuang, X.T. Wang, L. Zhang, L.Y. Tao, B. Lv, The effect of PDIA3 gene knockout on the mucosal immune function in IBS rats, Int. J. Clin. Exp. Med. 8 (2015) 6866–6877.

[58] N. Pishesha, T.J. Harmand, H.L. Ploegh, A guide to antigen processing and presentation, Nat. Rev. Immunol. 22 (2022) 751–764, https://doi.org/10.1038/s41577-022-00707-2.

[59] Q. Lu, et al., Potential of natural products in the treatment of irritable bowel syndrome, Phytomedicine : international journal of phytotherapy and phytopharmacology 106 (2022) 154419, https://doi.org/10.1016/j.phymed.2022.154419.

[60] J. Wang, et al., TRIM27 maintains gut homeostasis by promoting intestinal stem cell self-renewal, Cell. Mol. Immunol. 20 (2023) 158–174, https://doi.org/10.1038/s41423-022-00963-1.

[61] D. Bernardo, et al., T-cell proliferation and forkhead box P3 expression in human T cells are dependent on T-cell density: physics of a confined space? Hum. Immunol. 73 (2012) 223–231, https://doi.org/10.1016/j.humimm.2011.12.017.